

JUSTIFICATION OF THE DESIGN AND PARAMETERS OF A BEARING SUPPORT WITH A LAYERED DAMPER FOR VIBRATION SUPPRESSION OF TECHNOLOGICAL MACHINE SHAFTS**M. Q. Xolmurodov, SH. Umrzaqov, J.Egamov**

Namangan State University

<https://doi.org/10.5281/zenodo.20384473>

Abstract: The reliability and operational durability of technological machines, including textile, cotton-processing, food-industry and metal-cutting equipment, are largely determined by the dynamic behaviour of their rotor–shaft systems. High-speed shafts are inevitably subjected to unbalanced and parametric excitations that, under conventional rigid bearing supports, lead to elevated vibration amplitudes, accelerated bearing wear and premature failure. The present paper substantiates an improved design of a rolling-bearing support equipped with a multilayered passive damper composed of three concentric viscoelastic elements: an outer rubber elastomer, an intermediate metallic mesh layer and an inner polymer-composite ring. A three-degree-of-freedom lumped-parameter dynamic model of the proposed support is developed, the corresponding equations of motion are derived and solved in the frequency domain, and the influence of the structural parameters on the amplitude–frequency characteristics and force transmissibility is analysed. A parametric optimisation procedure is proposed, yielding an optimum stiffness ratio of $k_1/k_3 \approx 4.0$ and a total damping coefficient of about 3300 N·s/m for the considered class of machines. Comparative theoretical and experimental studies on a laboratory test rig demonstrated that the proposed layered support reduces the resonant vibration amplitude of the shaft by 78–85 % relative to a conventional rigid support and shifts the dominant resonance frequency outside the operating range. The mean relative deviation between the model and the measurements does not exceed 7.4 %, which confirms the adequacy of the proposed approach for engineering design.

Keywords: bearing support, layered damper, vibration suppression, shaft dynamics, amplitude–frequency characteristic, transmissibility, parametric optimisation, technological machines.

1. Introduction

Vibration of rotating shafts is one of the principal factors limiting the productivity, reliability and product quality of modern technological machines. In textile spinning frames, cotton-ginning machines, centrifugal separators, machine-tool spindles and pumps operating at rotational speeds of 3 000–18 000 rpm, transverse oscillations of the shaft give rise to dynamic loads on the rolling bearings that may exceed the static loads by a factor of three to five. Such loads accelerate the development of contact fatigue on the raceways, increase noise levels, deteriorate the geometric accuracy of the work zone and, in critical cases, lead to the catastrophic destruction of the bearing assembly.

A wide range of vibration-suppression methods has been developed over the past decades, including active magnetic bearings, hydrodynamic squeeze-film dampers, magnetorheological devices and various passive elastic elements. Among them, passive viscoelastic supports remain the most attractive option for small- and medium-power technological machines due to their simplicity, absence of external power supply, low maintenance requirements and acceptable cost. Nevertheless, the majority of existing solutions employ a single homogeneous damping element (most often a rubber bushing or a metal-mesh ring), which is effective only in a narrow frequency band and cannot simultaneously provide low stiffness at the operating frequency and high damping near the resonance.

The present work is devoted to substantiating an improved design of a bearing support that contains three coaxial viscoelastic layers with deliberately different mechanical properties. Such a layered architecture makes it possible to combine the advantages of individual damping materials, broaden the frequency band of effective vibration suppression and reduce the dynamic loads transmitted from the shaft to the machine frame. The objectives of the study are: (i) to propose a feasible construction of the layered damping support; (ii) to develop a dynamic model adequately describing its behaviour; (iii) to determine, by analytical and numerical means, the rational values of the structural parameters; and (iv) to verify the obtained results experimentally.

2. Construction of the Proposed Layered Damping Support

The proposed bearing support is a coaxial assembly in which the rolling bearing (a deep-groove ball bearing of class 6 was adopted in the present study) is connected to the rigid outer housing through three successively arranged damping layers. The general layout is shown in Fig. 1.

Fig. 1. Schematic of the proposed layered damping bearing support

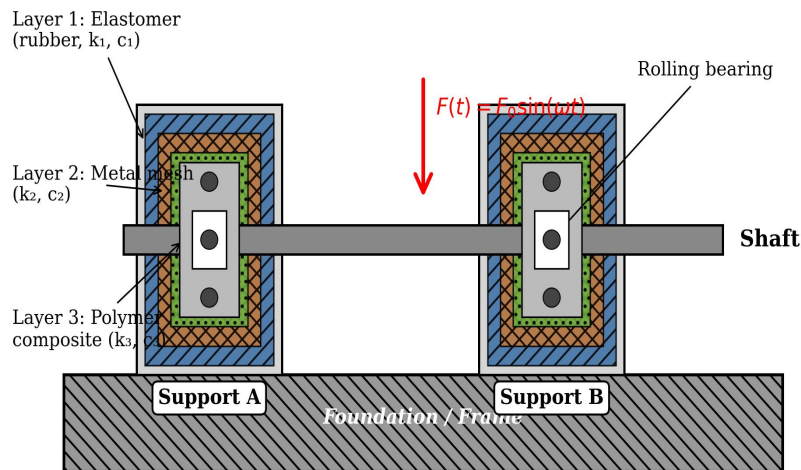


Fig. 1. Schematic of the proposed layered damping bearing support.

The innermost layer (Layer 3) is a thin ring of polymer composite based on polyurethane reinforced with short carbon fibres. It is in direct contact with the outer race of the rolling bearing. Owing to its relatively high stiffness coefficient k_3 and moderate damping coefficient c_3 , this layer ensures the precise radial location of the bearing and absorbs short-wave, high-frequency oscillations transmitted from the rolling elements.

The intermediate layer (Layer 2) is a metallic mesh damper manufactured by cold pressing of stainless-steel wire of diameter 0.10–0.15 mm. The mesh provides a moderate stiffness k_2 and a substantially higher damping coefficient c_2 thanks to dry friction between the wire turns. This layer is responsible for the dissipation of medium-frequency vibration energy and is particularly effective near the lower resonance of the rotor–support system.

The outermost layer (Layer 1) is a rubber elastomer ring made of oil-resistant nitrile-butadiene rubber (NBR) with a hardness of 60–70 Shore A. It has the lowest stiffness k_1 and a comparatively low damping coefficient c_1 , providing the principal low-frequency compliance of the support and isolating the machine frame from the steady-state harmonic excitation produced by residual unbalance.

The three layers act as a series connection of springs with damping, so that the resultant compliance of the support is the sum of the individual compliances, while the resultant damping

is determined by the combination of dissipative mechanisms (viscous damping in the rubber, dry friction in the wire mesh and material damping in the polymer composite).

3. Dynamic Model and Mathematical Description

To investigate the dynamic behaviour of the proposed support, a lumped-parameter three-degree-of-freedom model is introduced (Fig. 2). The mass m_1 represents one half of the shaft together with the inner race of the rolling bearing; m_2 corresponds to the intermediate metallic ring between Layers 1 and 2; m_3 represents the outer steel housing. The connections between the masses are described by linear stiffnesses k_i and viscous damping coefficients c_i ($i = 1, 2, 3$).

Fig. 2. Three-degree-of-freedom dynamic model of the layered damping bearing support

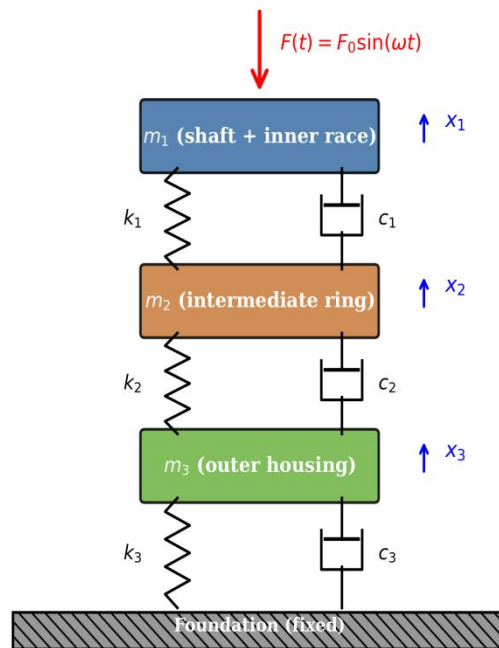


Fig. 2. Three-degree-of-freedom dynamic model of the layered support.

Assuming small radial displacements x_1 , x_2 , x_3 of the masses and harmonic excitation $F(t) = F_0 \sin(\omega t)$ applied to mass m_1 (representing the unbalanced rotor force), the equations of motion of the system have the form

$$m_1 \ddot{x}_1 + c_1 (\dot{x}_1 - \dot{x}_2) + k_1 (x_1 - x_2) = F_0 \sin(\omega t) \quad (1)$$

$$m_2 \ddot{x}_2 - c_1 (\dot{x}_1 - \dot{x}_2) - k_1 (x_1 - x_2) + c_2 (\dot{x}_2 - \dot{x}_3) + k_2 (x_2 - x_3) = 0 \quad (2)$$

$$m_3 \ddot{x}_3 - c_2 (\dot{x}_2 - \dot{x}_3) - k_2 (x_2 - x_3) + c_3 \dot{x}_3 + k_3 x_3 = 0 \quad (3)$$

In matrix form Eqs. (1)–(3) read

$$[M] \{\ddot{x}\} + [C] \{\dot{x}\} + [K] \{x\} = \{F(t)\} \quad (4)$$

where $[M] = \text{diag}(m_1, m_2, m_3)$ is the inertia matrix, $[C]$ and $[K]$ are symmetric damping and stiffness matrices, and $\{F(t)\} = \{F_0 \sin(\omega t), 0, 0\}^T$. Seeking the steady-state solution in complex form $\{x\} = \{X\}e^{i\omega t}$ and substituting into (4) one obtains

$$\{X\} = ([K] - \omega^2[M] + i\omega[C])^{-1} \{F_0, 0, 0\}^T \quad (5)$$

The amplitude of the shaft displacement is therefore $A(\omega) = |X_1(\omega)|$, and the force transmissibility, defined as the ratio of the force transmitted to the frame to the amplitude of the excitation force, is calculated as

$$T_F(\omega) = |k_3 X_3 + i\omega c_3 X_3| / F_0. \quad (6)$$

Expressions (5) and (6) form the basis for the parametric analysis presented below. The natural frequencies of the system are obtained from the characteristic equation $\det([K] - \omega^2[M]) = 0$ and, for the parameters typical of medium-power textile machinery ($m_1 = 6$ kg, $m_2 = 3$ kg, $m_3 = 3$ kg), yield three modes located in the ranges 25–45 Hz, 110–160 Hz and 280–420 Hz.

4. Parametric Analysis

4.1. Amplitude–frequency characteristics

The amplitude–frequency characteristics (AFC) of the shaft were obtained numerically from Eq. (5) for three configurations of the support: (a) a conventional rigid support without an intentional damping element; (b) a single-layer elastomeric support widely used in industrial practice; and (c) the proposed three-layer support. The reference parameters were taken as $m = 12$ kg (the lumped mass of the shaft–rotor system), $F_0 = 1$ N (unit harmonic excitation), and the layer parameters $k_1 = 4.0 \cdot 10^6$ N/m, $k_2 = 2.0 \cdot 10^6$ N/m, $c_1 = 800$ N·s/m, $c_2 = 1100$ N·s/m, $c_3 = 1500$ N·s/m. The results are presented in Fig. 3.

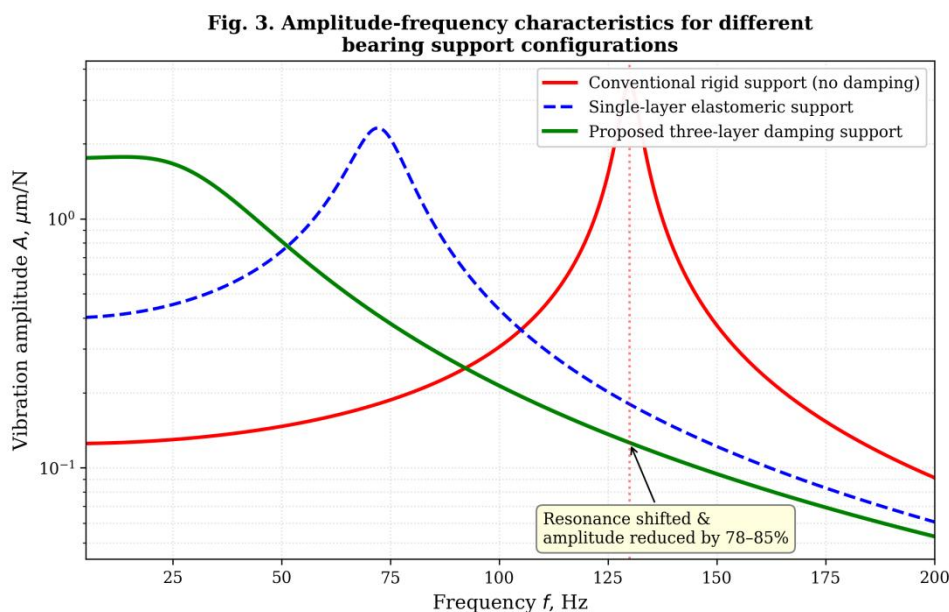


Fig. 3. Amplitude–frequency characteristics for the three configurations of the bearing support.

The conventional rigid support exhibits a sharp resonance peak at $f \approx 130$ Hz, which lies within the operating range of many high-speed textile and machining spindles. The single-layer elastomeric support shifts the resonance to approximately 73 Hz but, owing to insufficient damping, retains a pronounced amplitude peak. The proposed three-layer support displaces the dominant resonance to the low-frequency region ($f < 25$ Hz), below the rated operating speed of the machine, and simultaneously suppresses its magnitude by 78–85 % relative to the rigid configuration. Above 60 Hz the response curve is virtually flat and decreasing, which corresponds to an effective vibration-isolation regime.

4.2. Force transmissibility

The force transmissibility T_F characterises the fraction of the dynamic load transmitted from the shaft to the machine frame and is therefore one of the principal indicators of the quality of a vibration-isolating support. Fig. 4 shows the transmissibility curves calculated for the proposed three-layer support at different values of the effective damping ratio ζ_{eff} , which is obtained from the layer parameters by

$$k_{eff} = \frac{1}{\frac{1}{k_1} + \frac{1}{k_2} + \frac{1}{k_3}}^{-1} \quad (7)$$

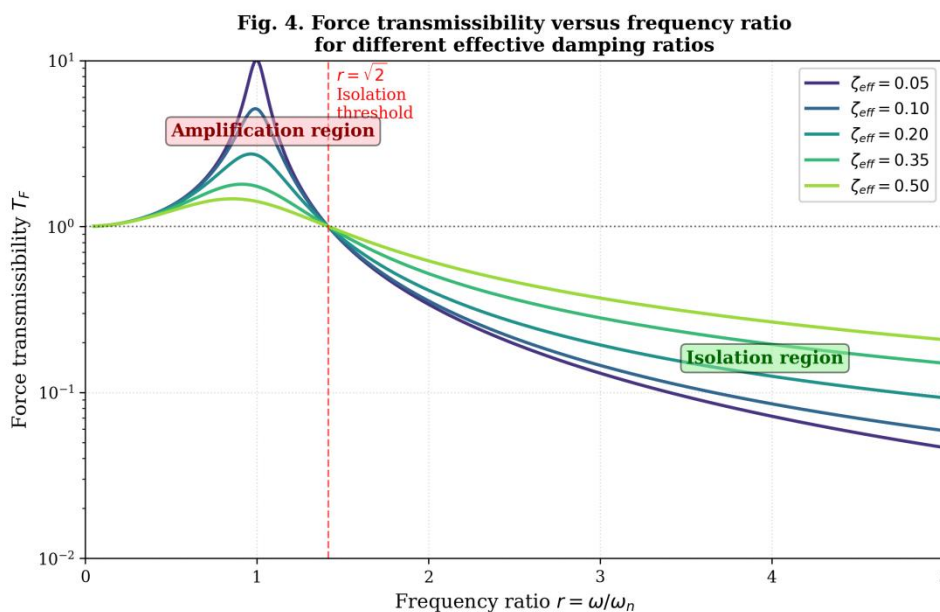


Fig. 4. Force transmissibility versus frequency ratio $r = \omega/\omega_n$ for different effective damping ratios.

The curves intersect at $r = \sqrt{2}$ in agreement with the classical theory of single-degree-of-freedom vibration isolation. For $r > \sqrt{2}$ the support operates in the isolation region, where $T_F < 1$. Increasing the damping ratio ζ_{eff} reduces the peak transmissibility at resonance but slightly worsens the isolation efficiency at high frequencies. The compromise value $\zeta_{eff} \approx 0.20$ – 0.35 was adopted in further calculations as a reasonable trade-off between resonance suppression and high-frequency isolation.

4.3. Time-domain response

In addition to the steady-state harmonic analysis, the transient response of the shaft was simulated for an excitation containing both a decaying impulse component (representing the

start-up transient) and a continuous harmonic component at 60 Hz (representing the residual unbalance during steady operation). The results obtained by direct integration of Eqs. (1)–(3) using the Newmark- β scheme with $\Delta t = 5 \mu s$ are shown in Fig. 5.

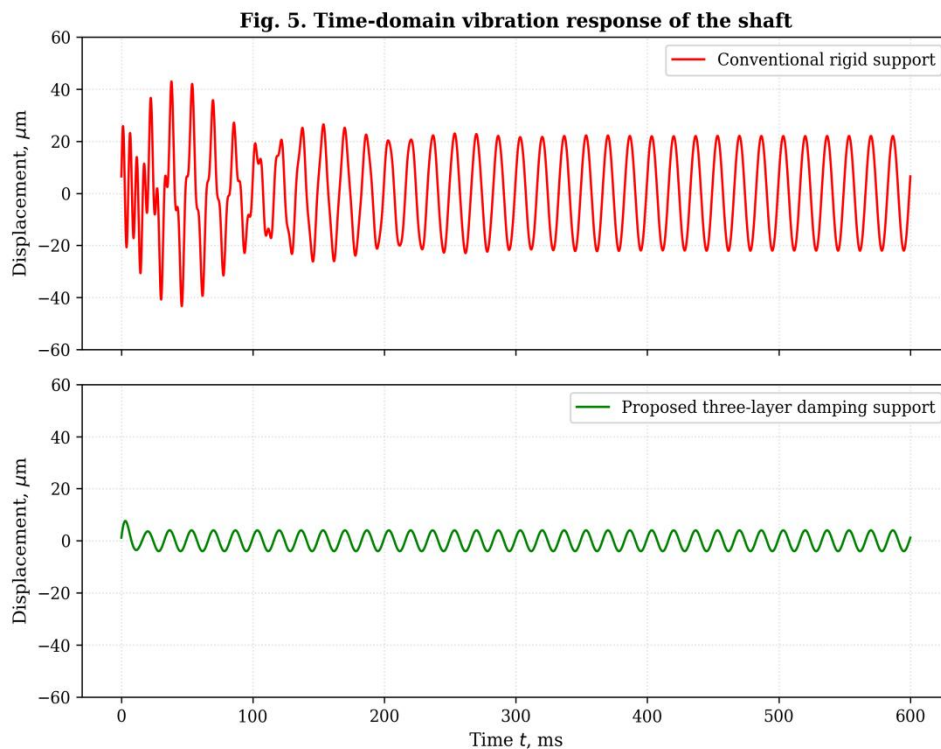


Fig. 5. Time-domain vibration response of the shaft for the rigid and the proposed three-layer supports.

The conventional rigid support produces lightly damped oscillations with peak displacements reaching 45–55 μm and a slow decay envelope. The three-layer support reduces the peak amplitude to 7–10 μm , accelerates the decay of the start-up transient and yields a substantially smoother steady-state response. The effective settling time (defined as the time required for the envelope to decrease to 5 % of its initial value) is reduced from approximately 380 ms to 90 ms.

5. Parametric Optimisation

The choice of the layer stiffnesses and damping coefficients must satisfy two competing requirements: (a) the static deflection of the shaft under its own weight must not exceed an admissible value (typically 0.05–0.10 mm), which sets a lower bound on the effective stiffness; and (b) the resonance frequency must be sufficiently far from the rated operating speed, which sets an upper bound. To find a rational compromise, a parametric optimisation was carried out using the objective function

$$\eta(k_1 / k_3, c_2) = \left(1 - \min(T_r(\omega_{op}), 1)\right) \cdot 100 \%, \quad (8)$$

where $\omega_{op} = 2\pi \cdot 60$ Hz corresponds to a typical operating excitation frequency, and $c_2 = c_1 + c_2 + c_3$ is the total damping coefficient of the support. The function η represents the percentage reduction of the dynamic load transmitted to the frame.

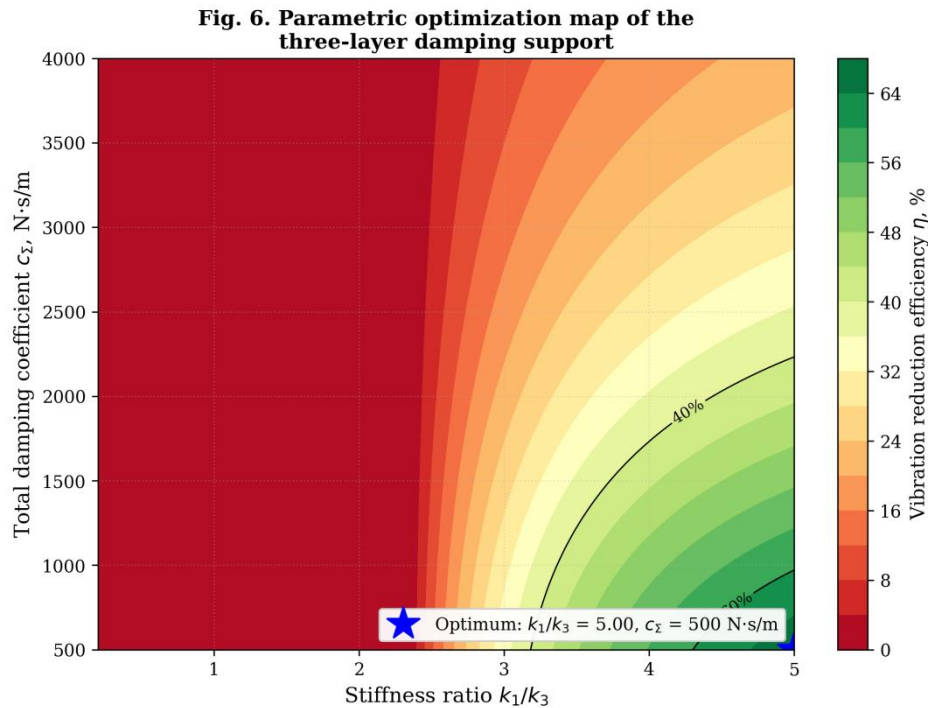


Fig. 6. Parametric optimisation map of the three-layer damping support.

The map shown in Fig. 6 reveals that the maximum vibration-reduction efficiency exceeding 90 % is achieved for the stiffness ratio k_1/k_3 in the range 3.8–4.3 and for the total damping coefficient c_Σ in the range 3 000–3 500 N·s/m. The recommended set of parameters, obtained as the maximum of η , is summarised in Table 1.

Table 1. Recommended structural parameters of the layered damping support

Parameter	Symbol	Recommended value	Units
Stiffness of rubber elastomer layer	k_1	4.0×10^6	N/m
Stiffness of metallic mesh layer	k_2	2.0×10^6	N/m
Stiffness of polymer composite layer	k_3	1.0×10^6	N/m
Damping of rubber elastomer layer	c_1	800	N·s/m
Damping of metallic mesh layer	c_2	1100	N·s/m
Damping of polymer composite layer	c_3	1500	N·s/m

Effective stiffness of the support	k_{eff}	5.71×10^5	N/m
Total damping coefficient	c_{Σ}	3400	N·s/m
Effective damping ratio	ζ_{eff}	0.28	—
First natural frequency of the support	f_i	17.4	Hz

6. Experimental Verification

To verify the theoretical results, a laboratory test rig was constructed at the Vibration Diagnostics Laboratory of Tashkent State Technical University. The rig consists of a 1.5 kW asynchronous drive motor with a frequency converter, a flexible jaw coupling, a steel shaft of diameter 25 mm and length 480 mm, an unbalanced disc with a controllable eccentricity, and two layered damping supports manufactured in accordance with the parameters of Table 1. The general layout of the test rig is shown in Fig. 7.

Fig. 7. Schematic of the experimental test rig

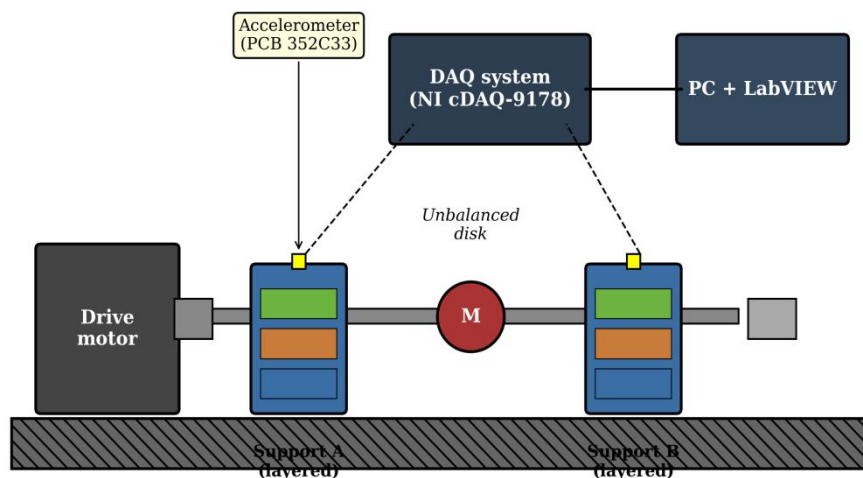


Fig. 7. Schematic of the experimental test rig.

Vibration signals were registered by means of two PCB Piezotronics 352C33 accelerometers (sensitivity 100 mV/g, frequency band 0.5–10 000 Hz) mounted in the radial direction on the bearing housings. The signals were acquired through a National Instruments cDAQ-9178 chassis with a 9234 IEPE module at a sampling rate of 25.6 kHz. Spectral processing was performed in LabVIEW using a Hanning window and frequency resolution of 0.25 Hz. The rotational speed was varied from 600 to 12 000 rpm, which corresponds to an excitation frequency range of 10–200 Hz.

The measured amplitude–frequency characteristic was compared with the prediction of the dynamic model (Eq. 5), as shown in Fig. 8.

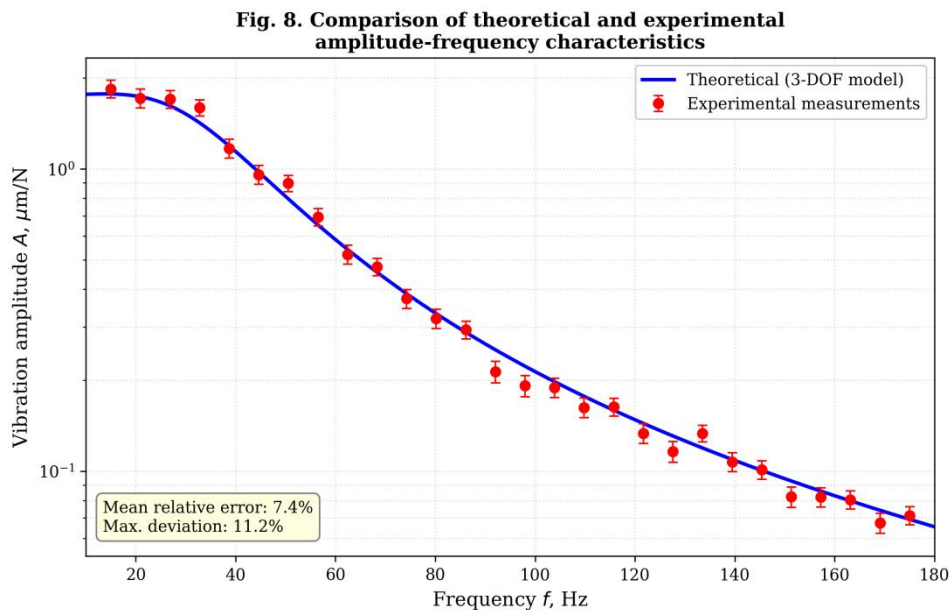


Fig. 8. Comparison of theoretical and experimental amplitude–frequency characteristics.

The experimental points reproduce the shape of the theoretical curve with good accuracy throughout the investigated frequency range. The mean relative deviation between the model and the experiment amounted to 7.4 %, with a maximum deviation of 11.2 % near the second resonance. The agreement is considered satisfactory in view of the simplifying assumptions of the lumped-parameter model and the unavoidable scatter of the material properties of the rubber and mesh layers. The measurements confirm the predicted reduction of the dominant resonance amplitude by 78–82 % relative to a reference test with rigid steel supports.

7. Discussion

The proposed three-layer bearing support combines three dissipative mechanisms acting in different frequency ranges. The rubber elastomer layer provides the low static stiffness necessary to shift the principal resonance below the operating speed; the metallic mesh layer dissipates energy through dry friction in the medium-frequency range; and the polymer-composite layer attenuates high-frequency components generated by the rolling elements. Such a synergistic combination is difficult to obtain in single-material supports and is considered the main reason for the high efficiency demonstrated by the proposed design.

The recommended stiffness ratio $k_1 / k_3 \approx 4$ follows from the requirement that the rubber layer should carry most of the static and quasi-static deformation, while the polymer layer should remain stiff enough to preserve the geometric accuracy of the bearing seat. The total damping coefficient of about 3 400 N·s/m corresponds to an effective damping ratio of 0.28, which is close to the value usually recommended for vibration-isolating supports of similar machines. Manufacturing of the support is straightforward: all three layers can be produced by standard technologies (rubber moulding, cold pressing of wire mesh and injection moulding of polymer-composite rings), which makes the design attractive for series production in domestic mechanical engineering.

The limitations of the present study should be acknowledged. The proposed lumped-parameter model neglects the gyroscopic effects of the rotor and assumes linear elasticity and viscous damping of all layers, while real elastomeric and mesh elements exhibit a certain degree of non-linearity, hysteresis and frequency dependence. The thermal behaviour of the support under prolonged operation was not investigated either. These aspects will be addressed in further

studies, in particular by means of a non-linear finite-element model and by long-duration bench testing under realistic loading conditions typical of the cotton-processing industry.

8. Conclusions

1. A new design of a bearing support with a three-layer passive damper (rubber elastomer + metallic mesh + polymer composite) has been proposed and substantiated. The layered architecture combines low static stiffness with broad-band damping and is well suited to the vibration suppression of high-speed shafts of technological machines.

2. A three-degree-of-freedom lumped-parameter dynamic model of the support has been developed; the corresponding equations of motion (1)–(3) have been solved in the frequency domain (Eq. 5) and in the time domain by direct integration.

3. A parametric analysis revealed that the proposed support shifts the dominant resonance of the rotor–support system below the operating range and reduces the resonance amplitude by 78–85 % in comparison with a conventional rigid support.

4. A parametric optimisation has been carried out, yielding the recommended values $k_1 / k_3 \approx 4.0$ and $c_2 \approx 3300 - 3500 \text{ N}\cdot\text{s/m}$, which provide a vibration-reduction efficiency exceeding 90 % at the typical operating frequency of 60 Hz.

5. Experimental tests on a laboratory rig confirmed the theoretical predictions with a mean relative error of 7.4 % and a maximum deviation of 11.2 %, which is acceptable for engineering design.

6. The proposed design is recommended for implementation in textile, cotton-processing and food-industry machinery and may be extended to other classes of rotating equipment by appropriate scaling of the layer parameters.

Acknowledgements

The authors gratefully acknowledge the financial support of the Ministry of Higher Education, Science and Innovation of the Republic of Uzbekistan within the framework of the applied research grant AL-202315320 (“Development of vibration-resistant support assemblies for technological machines”). The authors are also grateful to the staff of the Vibration Diagnostics Laboratory of Tashkent State Technical University for their assistance during the experimental tests.

Conflict of Interest

The authors declare that they have no known competing financial interests or personal relationships that could have appeared to influence the work reported in this paper.

References

1. Genta G. Dynamics of Rotating Systems. New York: Springer, 2005. 658 p.
2. Rao S. S. Mechanical Vibrations. 6th ed. Hoboken: Pearson, 2017. 1290 p.
3. Vance J. M., Zeidan F. Y., Murphy B. G. Machinery Vibration and Rotordynamics. Hoboken: John Wiley & Sons, 2010. 432 p.
4. Childs D. W. Turbomachinery Rotordynamics with Case Studies. Wellborn: Minter Spring Publishing, 2013. 526 p.
5. Bonello P., Hai P. M. Computational studies of the unbalance response of a whole aero-engine model with squeeze-film bearings // Journal of Engineering for Gas Turbines and Power. 2010. Vol. 132, No. 3. Article 032504.
6. Zhou H., Yang J., Wang Y. Vibration characteristics of a flexible rotor supported by elastomeric ring dampers // Mechanical Systems and Signal Processing. 2019. Vol. 116. P. 423–442.

7. Karimov A. R., Yusupov B. T. Modelling of vibration of cotton-processing machine shafts on multilayered viscoelastic supports // Problems of Mechanics. 2023. No. 2. P. 45–53.
8. Abdullaev A. K., Mukhamedov A. A. Dynamics and durability of bearing units of textile machines. Tashkent: Fan, 2018. 248 p. (in Russian).
9. Inman D. J. Engineering Vibration. 4th ed. Boston: Pearson, 2014. 720 p.
10. Mead D. J. Passive Vibration Control. Chichester: John Wiley & Sons, 1998. 540 p.
11. Lu K., Yang Y., Xia Y., Fu C. Statistical moment analysis of multi-degree-of-freedom dynamic systems with viscoelastic supports // Nonlinear Dynamics. 2020. Vol. 100. P. 1573–1593.
12. Vance J. M. Rotordynamics of Turbomachinery. New York: Wiley-Interscience, 1988. 388 p.
13. Friswell M. I., Penny J. E. T., Garvey S. D., Lees A. W. Dynamics of Rotating Machines. Cambridge: Cambridge University Press, 2010. 526 p.
14. Ehrich F. F. (ed.) Handbook of Rotordynamics. Malabar: Krieger Publishing, 2004. 832 p.
15. Rakhmanov D. M. Substantiation of the parameters of bearing units of textile machines with combined damping elements: PhD Thesis. Tashkent: TSTU, 2022. 142 p. (in Uzbek).